Periodico di Mineralogia (2015), 84, 3B (Special Issue), 633-655 DOI: 10.2451/2015PM0435

PERIODICO di MINERALOGIA
established in 1930

An International Journal of
MINERALOGY, CRYSTALLOGRAPHY, GEOCHEMISTRY,
ORE DEPOSITS, PETROLOGY, VOLCANOLOGY
and applied topics on Environment, Archaeometry and Cultural Heritage

U–Th–Pb "multi-phase" approach to the study of crystalline basement: application to the northernmost sector of the Ivrea-Verbano Zone (Alps)

Antonio Langone[1,*] and Massimo Tiepolo[2]

[1] C.N.R. - Istituto di Geoscienze e Georisorse, U.O.S. di Pavia, Via Ferrata 1, Pavia
[2] Dipartimento di Scienze della Terra "A. Desio", Università degli Studi di Milano, Via Botticelli 23, Milano
[*]Corresponding author: *langone@crystal.unipv.it*

Abstract

In situ U–Pb geochronology was carried out on amphibolites and siliciclastic metasediments of the Kinzigite Formation exposed in the northernmost sector of the Ivrea-Verbano Zone (Finero area). The aim is to shed light on the tectono-metamorphic evolution of this intermediate-lower crustal section and its bearing with the evolution of the southern and better known sectors of the Ivrea-Verbano Zone. Based on field observation and petrography, a metamorphic gradient gently increasing from amphibolite to upper amphibolite facies (from SE to NW) characterizes the whole metamorphic sequence. Granulite facies conditions are reached only by the slivers (septa) of the Kinzigite Formation into the External Gabbro unit of the Finero Mafic Complex. Metapelites consist mainly of biotite, quartz, plagioclase, garnet, and fibrolitic to prismatic sillimanite; muscovite progressively disappears as K-feldspar appears and becomes abundant. Amphibolites are made of green-brown hornblende and plagioclase and may contain clinopyroxene defining thin layers together with plagioclase and titanite. Both metapelites and amphibolites show mylonitic deformation which is more intense towards NW, i.e. towards the lower structural levels. The mylonitic deformation strongly affected the lower crustal metabasic rocks of External Gabbro unit (Finero Mafic Complex). Zircon, monazite and titanite U–Pb geochronology was carried out with laser ablation (LA)–ICP–MS on amphibolites, migmatitic paragneiss and septa. The multi-chronological approach allowed recognizing three discrete tectono-metamorphic events, at Permian, Triassic and Jurassic. Zircon and monazite yielded Permian ages suggesting (re) crystallization during an high temperature event characterized by both metamorphism and magmatism. Titanite dating provided Triassic and Jurassic ages, that were interpreted as U–Pb resetting ages. A Triassic perturbation of the U–Pb system was also recorded by zircon and monazite as rare domains.

The tectono-metamorphic reconstruction of the evolution of the northernmost Ivrea-Verbano Zone, as revealed by the new geochronological data, is only partially in agreement

with the temperature-time evolutions depicted for the southern sectors of the Ivrea-Verbano Zone. Permian ages indicating magmatism and high temperature metamorphism are common throughout the Ivrea-Verbano Zone, as well as the Jurassic ages related to local thermal pulses likely related to lithospheric thinning and associated lithospheric advection. Conversely, the occurrence of Triassic ages is peculiar of the Finero area. Two possible explanations may account for this Triassic event: Triassic ages are possibly related to the thermal effect and fluid circulation during the emplacement of the External Gabbro unit; or alternatively, they are the response to the ductile deformation largely recognized in the whole area. This study is a further evidence of the necessity of approaching crystalline basement with multiple geochronometers in order to unravel the complete tectono-metamorphic evolution.

Key words: U–Pb geochronology; LA–ICP–MS; Kinzigite Formation; Valle Cannobina; Ivrea-Verbano Zone.

Introduction

The U–Pb system in zircon is among the most used geochronometer to date high temperature events in crystalline basement (e.g. Vavra et al., 1996). Notwithstanding, interpretation of zircon dates is sometimes difficult, especially in poly-metamorphic rocks. The coupling of geochronological results with trace element geochemistry, and heavy rare earth elements (REE) in particular, may be efficient in detecting minerals stable with zircon (e.g. garnet) and in turn the metamorphic conditions. In some situations however, such as those occurring at almost constant high temperature during garnet stability (e.g. UHP), zircon fails to discriminate prograde from retrograde Pressure–Temperature (P–T) paths (e.g. Rubatto et al., 1999). Zircon, for its relatively high closure temperature, may also fail to date processes occurring at temperatures below the upper amphibolite metamorphic facies. Least but not last, zircon may be also present in very low amounts in mafic and ultramafic granulites and amphibolites, fact that limits its use as geochronometer.

The recent advances in microbeam techniques allowed geochronologists to carry out precise and accurate data in the U–Th–Pb system on a variety of minerals other than zircon such as monazite, titanite, rutile and apatite. Among these, monazite is certainly the most used mineral to date different stages of P–T paths (e.g. Langone et al., 2011 and references therein) for several reasons: low common Pb, high reactivity during metamorphic processes and slightly lower closure temperature relative to zircon, resulting suitable to date metamorphic events down to the lower amphibolite facies. Although titanite has a closure temperature similar to that of monazite (Cherniak, 1993), it is less used to date metamorphic processes for the higher contents in common Pb. Monazite is a widespread mineral of the metapelitic system but it is extremely limited in metabasites where titanite is a much more abundant accessory mineral (e.g. Frost et al., 2000). It follows that in complex crystalline basements the coupling of different geochronometers is a fundamental tool for reconstructing and deciphering in details the whole metamorphic evolution.

The Ivrea-Verbano Zone (IVZ), also referred to as the Ivrea Zone, in north-western Italy and southern Switzerland represents one of the most studied cross-section through the intermediate-lower thinned continental crust (down to 25 km, Demarchi et al., 1998). Even though it has been the focus of several petrological, geochemical, structural and geophysical studies (e.g. Bertolani, 1968; Zingg, 1983; Schmid et al., 1987; Handy and Zingg, 1991; Sinigoi et

al., 1994; Boriani and Villa 1997; Barboza and Bergantz, 2000, Redler et al., 2012; Ewing et al., 2013), the Temperature–time (T–t) evolution of the IVZ is still matter of debate (e.g. Ewing et al., 2013; Smye and Stockily, 2014). As pointed out by several authors (e.g., Schaltegger and Gebauer, 1999; Vavra et al., 1999), the evolution of the IVZ was characterized by distinct thermal and/or hydrothermal overprints suggesting that some geochronological data are likely biased by this event and only carry incomplete and disturbed information about regional metamorphism. Moreover, it has been recently demonstrated that the IVZ was affected also by local thermal perturbations linked to both magmatism and tectonic events (Zanetti et al., 2013; Smye and Stockily, 2014).

Here we apply a U–Th–Pb multi-chronological approach, based on U–Th–Pb geochronology of zircon, titanite and monazite, to the crystalline basement exposed in the Valle Cannobina (northern IVZ, Finero area) with the aim to better constrain the T–t evolution of this sector of the IVZ. The need of a petrological and geochronological update for the Kinzigite Formation exposed in Valle Cannobina is twofold. Despite the Kinzigite Formation has been the focus of numerous P–T–t reconstructions, these studies focused on the central/southern IVZ where the metamorphic pile reaches the maximum thickness and ductile/brittle deformation has weak effect. Moreover, recent works suggesting the occurrence of Triassic magmatism (Zanetti et al., 2013) in the Finero area imply the subdivision of the IVZ in at least two structurally different sectors. The new P–T–t data will provide new insights on the effective different tectono-metamorphic evolution of the northernmost sector of the IVZ.

Geological setting

The IVZ represents an uplifted part of the pre-Alpine intermediate-lower continental crust located in the southern Alps of northwest Italy (e.g. Schmid, 1993). It extends lengthwise for a distance of about 120 km and is bounded by two major fault zones, the Insubric Line in the northwest and the Cossato-Mergozzo-Brissago Line (CMBL) in the southeast (Figure 1A). The latter was active in the Permian and was reactivated also in more recent times (Boriani et al., 1990, Boriani and Villa, 1997; Mulch et al., 2002b). Locally, the CMB mylonites are crosscut and partially overprinted by mylonites of the Pogallo Line (PL; Figure 1A) which is interpreted as a low-angle normal fault due to crustal thinning (Hodges and Fountain, 1984), active during Early Mesozoic time (210-170 Ma, Zingg et al., 1990).

The southern part of the IVZ (e.g. Val Sesia) has been traditionally subdivided in three main lithological units: Kinzigite Formation (supracrustal metamorphic rocks), Mafic Complex (intrusive mafic rocks; Figure 1A) and mantle peridotite. These units show a SW-NE strike and a broad metamorphic gradient increase from amphibolite to granulite facies from SE towards NW (e.g. Schmid and Wood, 1976; Zingg, 1983; Schmid, 1993; Henk et al., 1997). The Kinzigite Formation occupies the south-eastern and originally the upper part of the tilted crustal section (Figure 1A) and consists of siliciclastic metasediments with intercalation of metabasic rocks and minor calcsilicate rocks and marbles. The most studied outcrops of the Kinzigite Formation are exposed in Val Strona di Omegna (Figure 1A) where the metasedimentary rocks show a continuous metamorphic gradient from amphibolite- to granulite-facies conditions (e.g. Henk et al., 1997). Granulites are not reported from other well-known outcrops (e.g. Val Sesia and Val Strona di Postua) except for a few septa (Quick et al., 2003). The siliciclastic metasediments evolve from schists to migmatites with increasing the metamorphic grade, i.e. from southeast to northwest, approaching to the

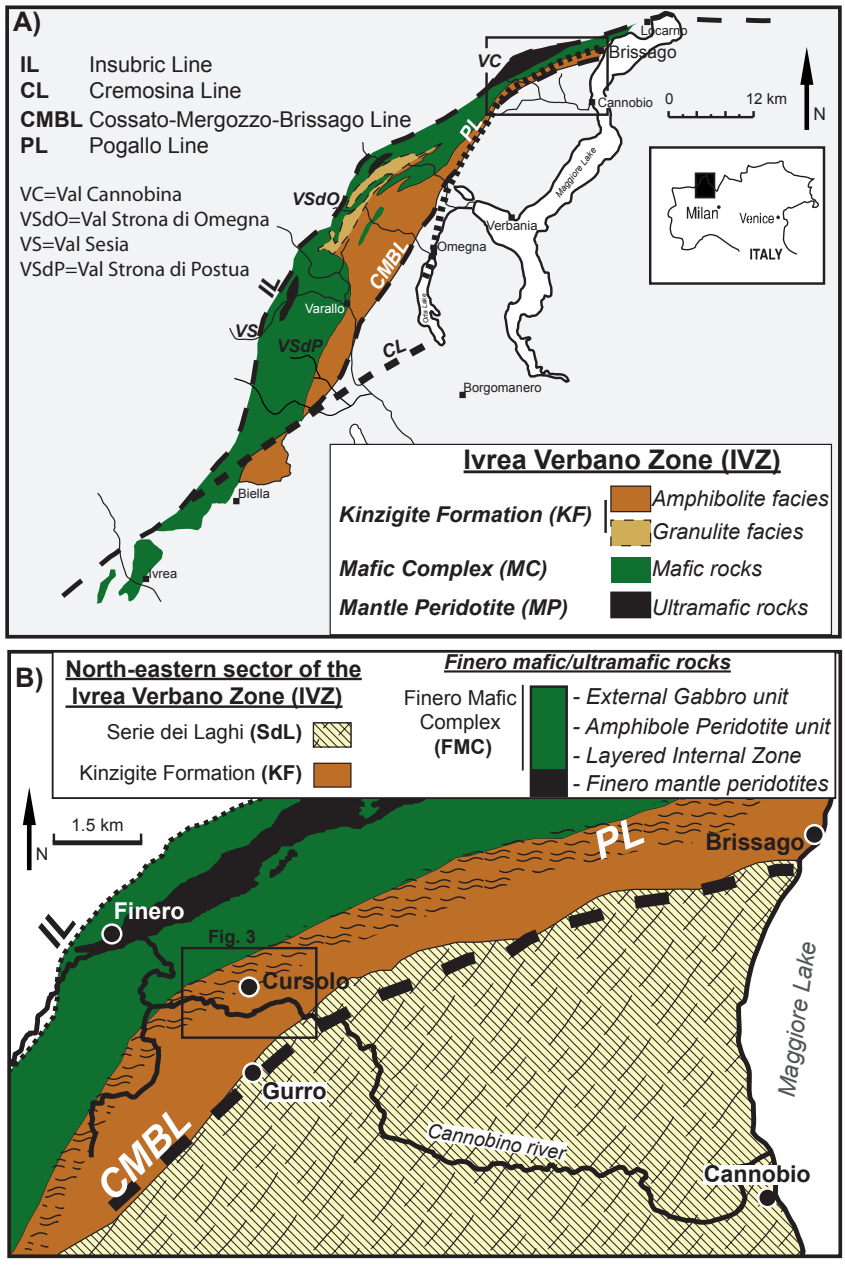

Figure 1. A) Sketch map of the Ivrea-Verbano Zone (westernmost part of the southern Alps) simplified after Zingg et al. (1990) and Boriani et al. (1990). Black box delimits the northeastern-most part of the IVZ. B) Schematic geological map of the north-eastern sector of the IVZ , modified after Boriani et al. (1990). Black box delimits the studied area which geological sketch map is shown in Figure 3.

Mafic Complex (Figure 1A). The regional mineral assemblages are overprinted by contact metamorphism in close proximity to gabbroic rocks of the Mafic Complex (e.g., Barboza and Bergantz 2000, Barboza et al., 1999; Redler et al., 2012).

The Kinzigite Formation structurally overlies the Mafic Complex (MC, Figure 1A) that was emplaced during Permian (e.g. Peressini et al., 2007) and consists of gabbro, norite and diorite and shows granulite facies metamorphic overprint (e.g. Rivalenti et al., 1975). The Mafic Complex in the central part of the IVZ is almost absent (Redler et al., 2012).

The northernmost sector of the IVZ (from the Valle Cannobina to Brissago) is characterized by mantle peridotites, intrusive crustal mafic to ultramafic rocks and supracrustal metamorphic rocks (Kinzigite Formation) as in the southern part but with peculiar features (Figure 1B). The Kinzigite Formation is less exposed with respect to mafic and ultramafic rocks of both mantle and crustal origins. Mylonites related to the CMBL and the PL are common and mark the contact between i) the Kinzigite Formation and upper-crustal metasediments of the Serie dei Laghi (SdL) and ii) the Kinzigite Formation and the mafic rocks (Boriani et al., 1990; Boriani and Burlini, 1995), respectively (Figure 1B). In Valle Cannobina the Kinzigite Formation shows another peculiarity, it is characterized by the presence of dike swarms ("Appinites" of Boriani and Sacchi, 1973) striking ENE-WSE and steeply dipping. These dikes range from hornblende-dioritic to granitic in composition (Boriani and Sacchi 1973; Boriani et al., 1990; Mulch et al., 2002b) and are intruded in both the IVZ and the SdL. Dikes occur sub-concordant with the main foliation and are preferentially localized within the mylonitic belt of the CMBL (Boriani and Sacchi 1973; Boriani et al., 1990; Mulch et al., 2002b). The relationship between deformation and dike emplacement are still unclear, dikes have been interpreted as post- mylonitic (e.g. Boriani et al., 1990; Boriani and Villa 1997) or syn-mylonitic intrusions (Mulch et al., 2002b) that locally promoted partial melting along the entire CMBL (Burlini and Caironi, 1988; Boriani et al., 1990; Mulch et al., 2002b).

The Mafic Complex in the northernmost sector of the IVZ (Finero area) is significantly different from its analogue in the southern part and for this reason it is called Finero Mafic Complex. According to Siena and Coltorti (1989), it consists of three different units: i) the Layered Internal Zone (garnet-hornblendite, pyroxenites, anorthosites and garnet-gabbros); ii) the Amphibole Peridotite and iii) the External Gabbro, which is in contact with the Kinzigite Formation (Figure 1B). Recent U–Pb zircon geochronology yield a Triassic intrusion age for the External Gabbro (Zanetti et al., 2013). Slivers or lenses (< 1 m to 100 m thick) of the Kinzigite Formation occur within the External Gabbro unit and are generally referred to be *septa* (e.g. Sinigoi et al., 1994; 1996).

The Finero mantle peridotites are in contact with the Finero Mafic Complex and mostly consist of a pervasively metasomatized spinel-harzburgites which contain abundant phlogopite and amphibole (Zanetti et al., 1999).

Geochronological background

Despite the growing number of geochronological studies, the timing of magmatism and metamorphism within the IVZ is still matter of debate. A detailed geochronological review of the IVZ is not the aim of the present work. Here we report a summary of the U–Pb geochronological data concerning the Kinzigite Formation, the Mafic Complex and the Finero Mafic Complex, which are pertinent for the present study.

According to literature, two spatially and temporally major events of mafic magmatism interested the lower crustal segment of the IVZ: i) during Permian (295-280 Ma, U–Pb zircon data) in the southern/central IVZ (Peressini et

al., 2007 and references therein) and ii) during Triassic (232±3 Ma) of the IVZ northernmost sector (Finero area, Zanetti et al., 2013; Figure 2).

The thermal history of the Kinzigite Formation is characterized by multiple temperature pulses from Carboniferous to the Jurassic (Figure 2). Ewing et al. (2013) recently suggested that the regional amphibolite to granulite facies metamorphism occurred at 316±3 Ma (U–Pb is also consistent with U–Pb monazite cooling ages determined by Henk et al. (1997) and ranging between 292 and 276 Ma. Coherently, Vavra and Schaltegger (1999) interpreted an upper intercept U–Pb monazite age at about 293 Ma as cooling age. During Permian the upper part of the Kinzigite Formation exposed in the northern sector of the IVZ (Figure 1B) was affected by dike magmatism as documented

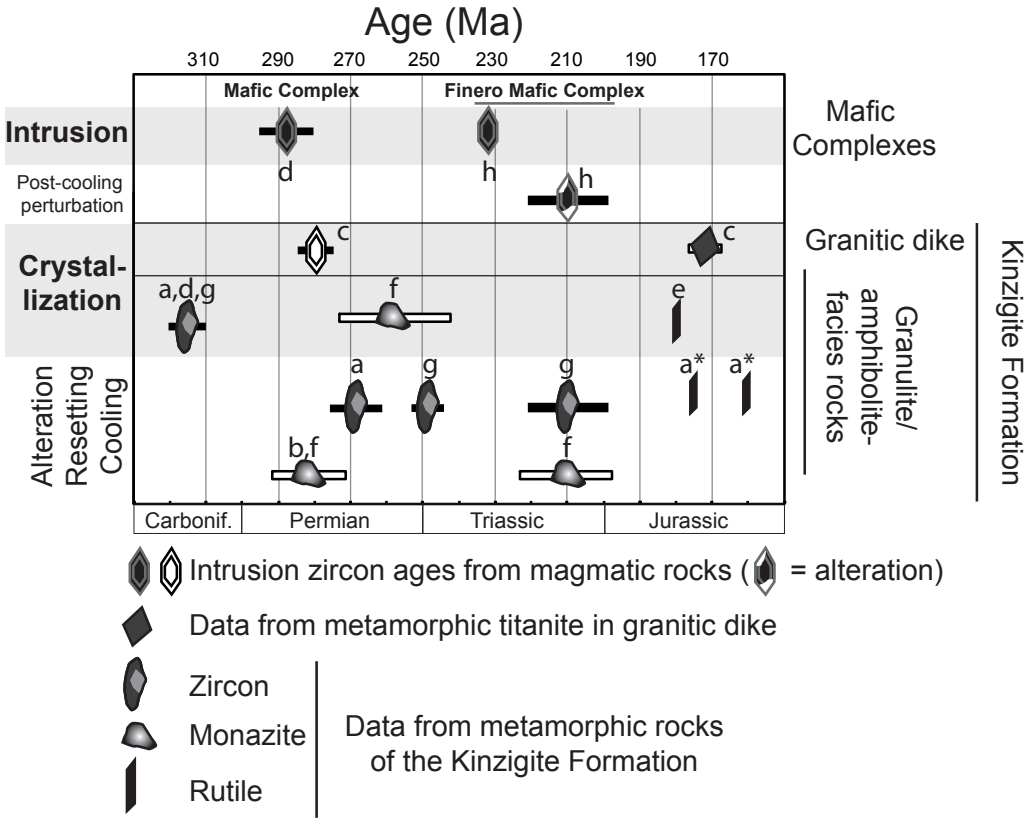

Figure 2. Summary of published U–Pb data of zircon, monazite, titanite and rutile from magmatic and metamorphic rocks of the Mafic Complex, the Finero Mafic Complex and the Kinzigite Formation. Bars indicate errors associated to the geochronological data. For a more complete summary providing geochronological data from other methods (e.g. Ar/Ar, Rb/Sr, Sm/Nd) see Zanetti et al. (2013). a) Ewing et al. (2013); a*) Ewing et al. (2015); b) Henk et al. (1997); c) Mulch et al. (2002b); d) Peressini et al. (2007); e) Smye and Stockli (2014); f) Vavra and Schaltegger (1999); g) Vavra et al. (1999); h) Zanetti et al. (2013).

central-southern IVZ. They were interpreted by the authors as recrystallization or age resetting events. According to Vavra and Schaltegger (1999) stages of post-cooling growth of new monazite crystals from metapelites occurred between 273 and 244 Ma. A thermal and/or decompression event close to the Permian/Triassic boundary was suggested by Vavra et al. (1999) based on a zircon population from granulites characterized by alteration features and a mean age of 249±7 Ma. As proposed by the authors, the same regional event was probably recorded also by other isotopic systems (e.g. Sm-Nd internal isochron by Voshage et al., 1987; Ar–Ar hornblende by Boriani and Villa, 1997).

Several geochronological data from both zircon and monazite suggest that the Triassic-Jurassic boundary was characterized by an important thermal perturbation. Mantle rocks and the lowest crustal levels in the northern sector of the IVZ were affected by widespread metasomatic events and pegmatite intrusions, respectively (e.g. Schaltegger et al., 2015 and references therein). Vavra et al. (1999) reported zircon rejuvenation within granulites at 210±12 Ma that they associated to the ingression of fluid related to the hydrothermal activity. SHRIMP U–Pb data on zircon rims from the External Gabbro exposed in Valle Cannobina yielded slightly U–Pb discordant data between 219±3 and 205±3 Ma (Zanetti et al., 2013) and were interpreted by the authors as the result of fluid assisted recrystallization, concomitant with the injection of alkaline melts forming discordant dikes and sills. U–Pb analyses of single monazite grains from granulitic metapelites performed by Vavra and Schaltegger (1999) revealed a lower intercept age of 210±14 Ma that was interpreted by the authors a fluid–driven Pb–loss.

Whilst Triassic-Jurassic boundary is mainly recorded as altered domains by fluid circulation, the Jurassic time is at present documented by the subsolidus crystallization of titanite and rutile. Mulch et al. (2002b) reported a metamorphic titanite growth at 173±4 Ma (TIMS U–Pb concordant data) from an hornblende-dioritic enclave within a composite dike along the CMBL in the northernmost sector of the IVZ. Recently, Smye and Stockly (2014) performed rutile U–Pb age depth profiles from granulite facies metasediments from the central IVZ (Val d'Ossola, Figure 1A). They obtained Jurassic $^{206}Pb/^{238}U$ ages that were related to a brief thermal pulse experienced by the IVZ plausibly associated with hyperextension. According to Ewing et al. (2015) the Jurassic history of the IVZ was characterised by two distinctive cooling stages (≈160 and 175 Ma; $^{206}Pb/^{238}U$ ages) recorded by rutile grains within granulite facies metapelites from throughout the former base of the IVZ.

Summing up (Figure 2), the available U–Pb geochronological data from different geochronometers suggest two main subsolidus crystallization events for the Kinzigite Formation at Carboniferous and Jurassic time. Even though Permian U–Pb ages of new monazite grains were reported, in this period both zircon and monazite developed domains suggesting alteration, resetting and cooling. Analogously, U–Pb data from upper Triassic to lower Jurassic derive from altered domains due to fluid circulation.

Studied area and petrography

A detailed structural and geological mapping was carried out in a small area around the Cursolo village (Valle Cannobina, Figure 3). Here, metamorphic rocks of the Kinzigite Formation and the Finero Mafic Complex show a SW-NE strike and are steeply dipping towards NW. The south-eastern sector is dominated by siliciclastic metasediments whereas amphibolites prevail in the north-western zone; several samples representative of the exposed lithologies were collected along SE-NW profiles. Amphibolites from the Kinzigite Formation are in contact with

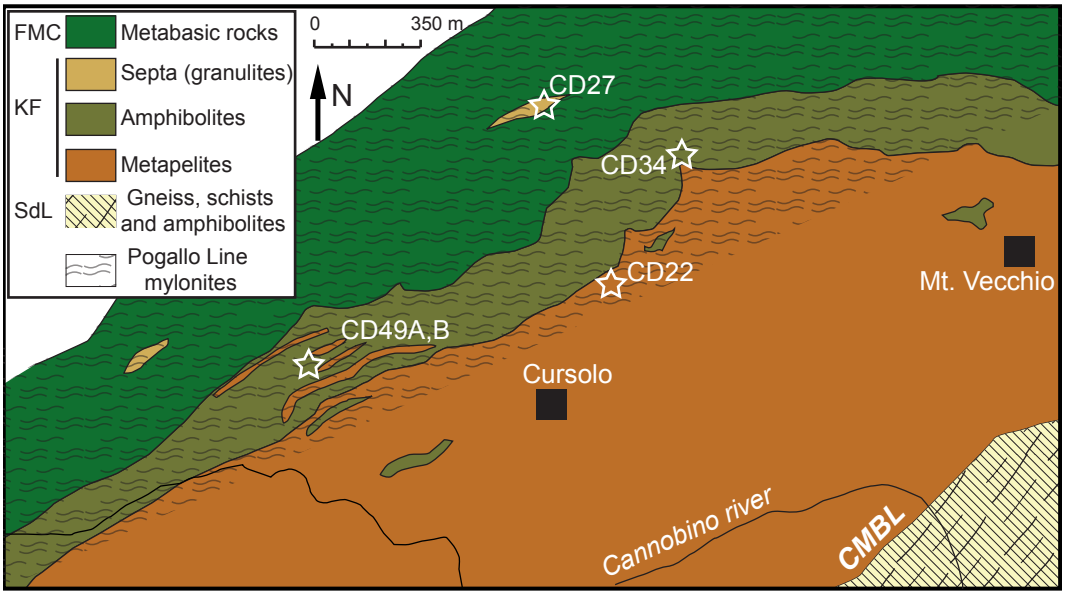

Figure 3. Geological sketch map of the studied area, around the Cursolo village (Valle Cannobina). White unfilled stars indicate locations of studied samples.

the External Gabbro unit of the Finero Mafic Complex showing amphibolite to granulite facies metamorphism (Figure 3). The distinction between amphibolites from the Kinzigite Formation and metamorphic rocks of the External Gabbro unit is sometimes difficult in the field. However, it is easily done in thin section based on the occurrence of orthopyroxene, which characterizes only the External Gabbro unit. The rocks of the Kinzigite Formation are bounded by two mylonitic shear zones. Towards SE, the contact between the metapelites of the Kinzigite Formation and the metasediments of the SdL is characterized by a mylonitic belt, belonging to the CMBL (Figure 1B and 3, Boriani and Sacchi, 1973). Several small dikes concordant/sub-concordant with respect to the mylonitic foliation were found along the CMBL but they are not reported in the geological map of Figure 3. According to Boriani et al. (1990) and Mulch et al. (2002b), these dikes intruded during Permian, promoted local partial melting and recorded a metamorphic overprint during Jurassic. Towards NW, mylonites mark the contact between metabasic rocks of the External Gabbro unit and the metamorphic rocks of the Kinzigite Formation. Septa derived from both amphibolite and metapelites are found within the External Gabbro unit of the Finero Mafic Complex (Figure 3). They show a well-developed mylonitic recrystallization. Brittle deformation is common and mainly overprints mylonitic rocks of both shear zones.

Based on field observations and mineral assemblages, the metapelites show a metamorphic gradient increasing from SE towards NW. With the increasing of the metamorphic grade, several features are observed: i) the modal abundance of garnet increases at the expense of that of biotite; ii) sillimanite progressively changes habitus from fibrolitic to prismatic; iii) (prograde) muscovite disappears as the K-feldspar

becomes abundant. Towards the contact with amphibolites (NW), siliciclastic metasediments define a narrow band of migmatites. They are characterized by quartzofeldspathic leucosomes and melanosomes dominated by garnet, biotite and sillimanite. The migmatites show a well developed mylonitic fabric characterized by anastomosing layers, of both leucocratic and melanocratic appearance, surrounding large garnet porphyroclasts (Figure 4A). Amphibolites consist of (green/brown) hornblende, clinopyroxene, plagioclase,±quartz±biotite, thus suggesting upper amphibolite facies conditions and locally partial melting (e.g. Kunz et al., 2014). Hornblende-rich and plagioclase-rich amphibolites are recognized and alternate at the outcrop scale. The hornblende-rich amphibolites consist mainly of hornblende (up to 90 vol %) with minor quartz and plagioclase defining lenses and/or thin layers (Figure 4B). Clinopyroxene occurs as small grains and together with plagioclase defines narrow bands

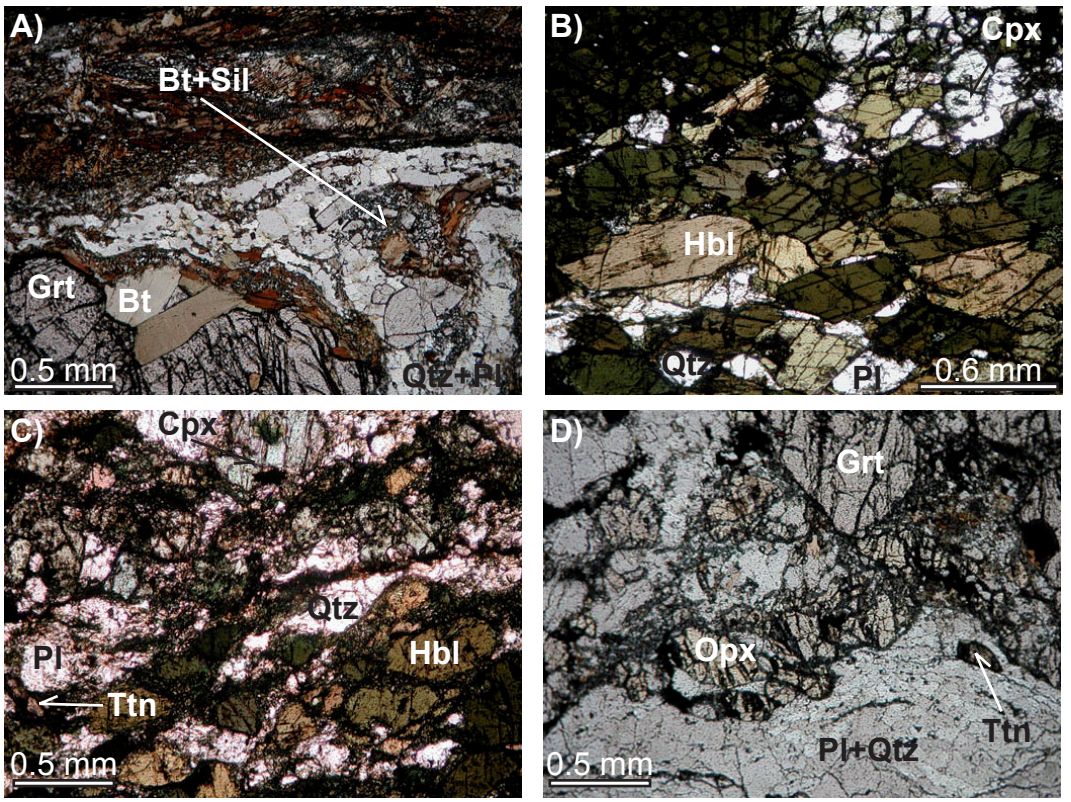

Figure 4. A) CD22 migmatitic metapelite: rim of a sub-rounded garnet porphyroclast partially replaced by biotite and wrapped by quartz+plagioclase leucosome. Biotite and sillimanite define layers and/or aggregates. B) CD1 hornblende-rich amphibolites with clinopyroxene; C) CD34 plagioclase-rich amphibolites; D) CD27 granulite facies mafic septa consisting of garnet, Ca-rich plagioclase, orthopyroxene, clinopyroxene and biotite. Quartz, together with plagioclase, defines layers and show dynamic recrystallization. Titanite is abundant, partially replaced by oxides and deformed. Mineral abbreviations follow Kretz (1983).

(Figure 4B) that appear greenish/light green at the hand specimen. The plagioclase-rich amphibolites consist of plagioclase, hornblende, quartz, clinopyroxene and minor titanite (Figure 4C). The latter forms layers or aggregates together with oxides and is observed either as separate grains or else rimming ilmenite. Similar features were observed by Kunz et al. (2014) for the amphibolites exposed in Val Strona di Omegna (central IVZ) and were interpreted by the authors as melt segregations during partial melting. Mylonitic deformation weakly overprints amphibolites whereas it strongly affects the External Gabbro unit of the Finero Mafic Complex. The mylonitic deformation promoted grain size reduction of amphibole and pyroxene grains and the development of fine grained mylonitic planes, locally ultramylonitic. Garnet becomes more abundant close to slivers of the metamorphic rocks (i.e. septa), originally belonging to the Kinzigite Formation and partially digested by the crystallizing mafic magma. In the studied area, septa consist of garnet, anorthitic-rich plagioclase, clinopyroxene and orthopyroxene, with minor biotite and quartz, (Figure 4D). Garnet is the dominant mineral phase. It occurs as large crystals partially replaced toward the rim by a fine grained symplectite similar to those reported by Kunz et al. (2014) in the metabasites from the Val Strona di Omegna. Titanite and rutile are accessory minerals. Titanite can reach dimensions up to 0.7x0.4 mm and is present both within the matrix and as inclusion within garnet. Rutile is absent in the matrix whereas commonly occurs in garnet, where it forms small long acicular or stubby crystals. Locally, rutile is replaced by Fe-Ti oxides, especially along or near cracks. Mafic granulites showing comparable peak mineral assemblages are reported in the Val Strona section (Figure 1A, e.g. Harlov and Förster, 2002a, 2002b). Mafic septa, coherently with respect to their host rocks, are also characterized by a well developed mylonitic fabric.

Five samples representative of the different lithologies of the Kinzigite Formation in the Cursolo area were selected for the geochronological investigations (Figure 3): one migmatitic metapelite (CD22), two plagioclase-rich amphibolites (CD34 and CD49A), one hornblende-rich amphibolite (CD49B) and one septa (CD27).

U–Th–Pb geochronology Methods

U–Th–Pb geochronology was carried out on zircon, monazite and titanite. Zircon was investigated only in the septa and in the amphibolites, rocks of the Kinzigite Formation showing the higher metamorphic grade in the studied area. Geochronological information from zircon of micaschists and migmatites of the Kinzigite Formation were retained not useful for the present work. The temperatures recorded by these rocks were likely unable to promote zircon recrystallization. Zircon grains were separated with conventional methods from the septa (CD27) whereas two zircon grains were analysed directly in thin section in the hornblende-rich amphibolite sample (CD49B). Titanite crystals were analysed in both the septa (CD27) and the plagioclase-rich amphibolites (CD34 and CD49A) directly in thin section. Monazite crystals were found only in the migmatite (CD22) and were analysed directly in thin section.

U–Th–Pb geochronology was carried out at the CNR-IGG UOS of Pavia with Laser Ablation (LA)–ICP–MS. The system couples an ArF excimer laser microprobe (type GeoLas102 from MicroLas) with a sector field ICP–MS (type Element from ThermoFinnigan). The analytical methods for zircon and monazite geochronology are described in details in Tiepolo (2003) and Paquette and Tiepolo (2007), respectively. The signal of ^{202}Hg, ^{204}(Pb+Hg), ^{206}Pb, ^{207}Pb, ^{208}Pb, ^{232}Th and ^{238}U masses were acquired. ^{202}Hg is acquired to correct the isobaric interference of

^{204}Hg on ^{204}Pb, so that the presence of common Pb in the sample can be monitored. However, the background of mass 204 is relatively high, due to trace of Hg in the He gas, and does not allow to appreciate small amounts of common Pb. Remarkably, in the investigated samples the signal of ^{204}(Pb+Hg) was always indistinguishable from the background. The ^{235}U signal is calculated from ^{238}U on the basis of the ratio ^{238}U/^{235}U = 137.818 (Hiess et al., 2012).

U–Pb fractionation effects in zircon and monazite were simultaneously corrected using a matrix matched external standard and considering the same integration intervals on the standard and the unknowns. For U–Th–Pb geochronology of zircon analyses were carried out using a spot size of 20 microns and a laser fluence of 10 Jcm^{-2}. The reference zircon GJ-1 (Jackson et al., 2004) was adopted as external standard and the reference zircon 91500 (Wiedenbeck et al., 1995) was selected as validation standard. For U–Th–Pb geochronology of monazite spot size was reduced to 10 microns. The Moacir monazite (Seydoux-Guillaume et al., 2002a, 2002b; Gasquet et al., 2010) was adopted as external. For titanite a spot size of 20 micron was used with a fluence of 10Jcm^{-2}. No matrix matched standards were available for titanite and thus we adopted zircon GJ-1 as external standard. According to Storey et al. (2006), the error related to the non-matrix-matching between the unknown and the external standard is negligible. However, more recent studies (e.g. Sun et al., 2012) suggest that errors up to 12% may be introduced dating titanite using zircon as external standard.

Data reduction was carried out with the software package GLITTER® (van Achterbergh et al., 2001). Individual uncertainties given by the software for the isotope ratios were propagated relative to the respective reproducibility of the standard. This procedure was carried out for each analytical run as reported in Horstwood et al. (2003). U–Pb data are plotted as Tera-Wasserburg diagrams (Tera and Wasserburg, 1972) with the ISOPLOT/Ex 3.00 software package by Ludwig (2003).

Results

Zircon geochronology

The heavy mineral separate from the septa sample (CD27) yielded only one zircon grain of about 80 microns wide. Under cathodoluminescence (CL) this grain does not show evident zoning (Zrc6; Figure 5A). Analyses were carried out in the two different domains and yield U–Pb concordant results at 275±11 Ma and at 230±8 Ma (Figure 5B; Table 1).

In the hornblende-rich amphibolite sample (CD49B) two zircon grains were found in thin section. One zircon is about 0.12 mm and under CL reveals a complex zoning pattern characterised mainly by oscillatory zoning with brighter irregular CL domains at the rims or defining narrow veins (Figure 5A); the other is smaller and is rather homogeneous. Three analyses were carried out on both zircon grains: the first one with oscillatory zoning (analyses Zrc1a-c, Table 1) yields one concordant date at 284±14 Ma that together with the other two discordant date provide a lower intercept date at 284±18 Ma (Figure 5B); the three analyses from the second grains (Zrc2a-c, Table 1) resulted discordant with ^{206}Pb/^{238}U date ranging from 280 to 286 Ma. In both zircon grains, the discordant data possibly reflect various amounts of common Pb and fluid induced alterations/resetting as suggested by the brighter irregular CL domains at the rims or defining narrow veins (e.g. Zrc1; Figure 5A).

Monazite geochronology

In the migmatitic metapelite monazite is mostly found in textural equilibrium with other matrix forming minerals, as inclusion within biotite flakes and in a few cases as inclusion within garnet. A cluster of monazite grains within biotite+sillimanite selvage (Mnz2a-d;

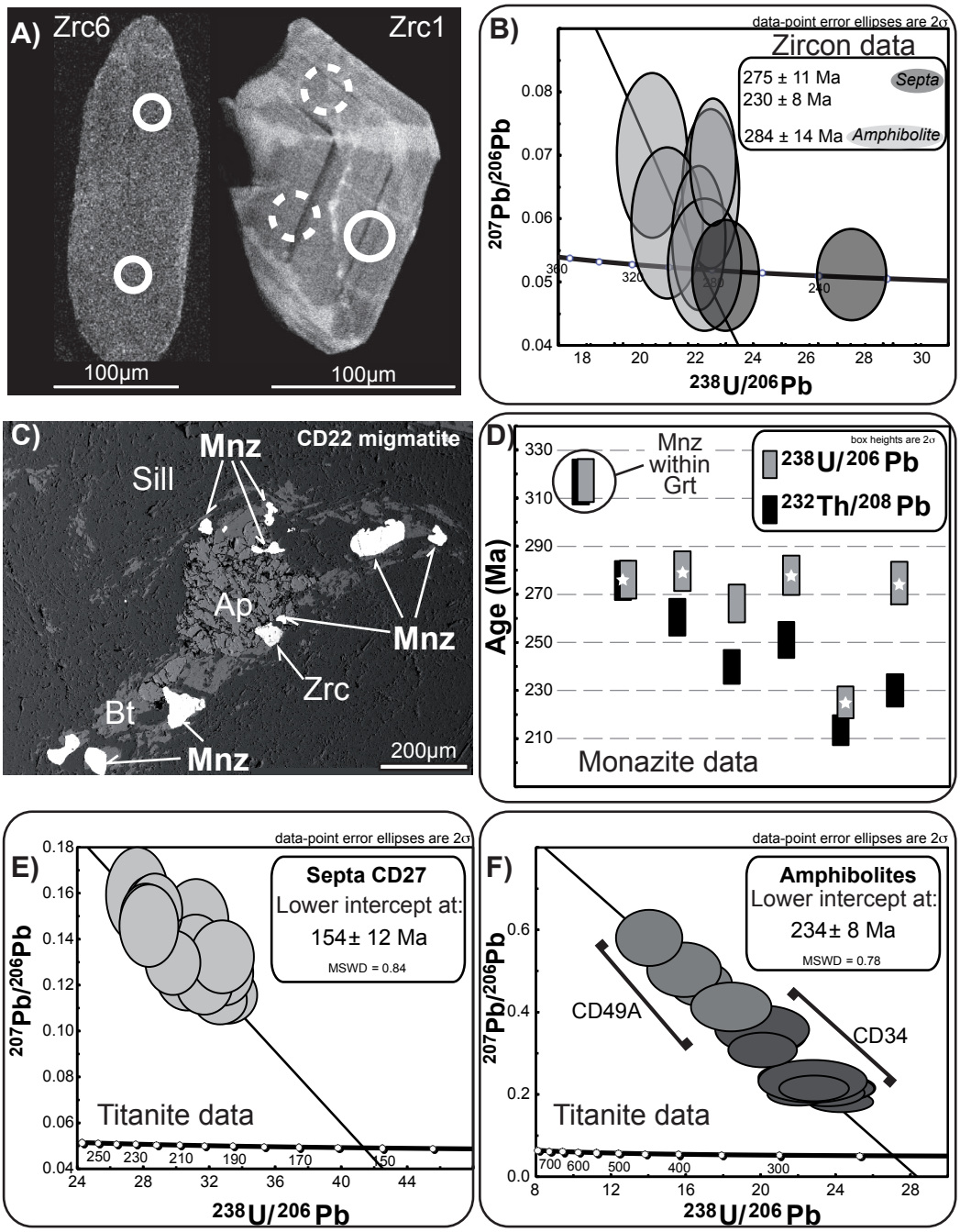
A)
Zrc6
Zrc1
100µm
100µm
B)
data-point error ellipses are 2σ
Zircon data
275 ± 11 Ma
230 ± 8 Ma
Septa
284 ± 14 Ma
Amphibolite
207Pb/206Pb
238U/206Pb
C)
CD22 migmatite
Mnz
Sill
Ap
Mnz
Zrc
Bt
Mnz
200µm
D)
box heights are 2σ
Mnz within Grt
238U/206 Pb
232Th/208 Pb
Age (Ma)
Monazite data
E)
data-point error ellipses are 2σ
Septa CD27
Lower intercept at:
154± 12 Ma
MSWD = 0.84
Titanite data
207Pb/206Pb
238U/206 Pb
F)
data-point error ellipses are 2σ
Amphibolites
Lower intercept at:
234± 8 Ma
MSWD = 0.78
CD49A
CD34
Titanite data
207Pb/206Pb
238U/206 Pb

Figure 5C; Table 1) and one grain included in garnet (Mnz1, Table 1) were selected for U–Th–Pb geochronology. Crystals are generally anhedral with rounded to sub-rounded shapes (Figure 5C) and back-scattered electrons images do not reveal significant zoning. The dimensions of two grains in the matrix allowed multiple analyses that were performed at different internal positions of the crystals (Table 1).

The monazite grain included in garnet shows a relatively robust concordant $^{206}Pb/^{238}U$–$^{208}Pb/^{232}Th$ date at 317±5 Ma (Figure 5D). The discordance of the $^{207}Pb/^{235}U$ date is most likely in relation to small amounts of common Pb. With one exception monazite grains in the matrix show discordant $^{206}Pb/^{238}U$–$^{208}Pb/^{232}Th$ dates. The exception is the one analysis of Mnz2a grain, which yields fully U–Th–Pb concordant data at 276±4 Ma (Figure 5D). The majority of the U–Pb dates in the other grains are concordant and yield a weighted average $^{206}Pb/^{238}U$ date at 277±4 Ma (4 analyses) with a Mean Squared Weighted Deviates (MSWD) of 0.26. Only one rim furnished a significantly younger date at 225±7 Ma. The $^{208}Pb/^{232}Th$ dates of monazite in the matrix yield scattered values between 260±8 Ma and 213±6 Ma with no clear relation with core/rim positions (Figure 5D).

Titanite geochronology

Twelve titanite crystals from the septa (CD27) were analysed and more than one spot per grain was randomly carried out. No concordant U–Pb data were obtained (Table 1). Although the signal of mass 204 was not discriminable from the background, all the analyses show the presence of variable contents of common Pb as revealed by the array of data in the Tera-Wasserburg diagram (Figure 5E). Correction for common Pb was carried out according to the method of Compston (1999) by fitting the array and considering the lower intercept date as representative of the (re)crystallization age. This approach yield for the septa a lower intercept date of 154±12 Ma (16 data; MSWD = 0.84).

Eleven titanite crystals (for a total of twelve analyses) were analysed for the plagioclase-rich amphibolite sample CD34 and three grains (for a total of four analyses) for the plagioclase-rich amphibolite sample CD49A. All data resulted discordant (Table 1) but, as in the previous case, the alignment in the Tera-Wasserburg diagram (Figure 5F) suggests discordance in relation to variable contents of common Pb. Regression of data points yields a lower intercept date at 234±8 Ma (MSWD = 0.78).

Discussion: Evidence for the occurrence of three discrete HT events

The paucity of zircon in the studied rocks causes a relatively limited statistical validity for

Figure 5. A) CL images of zircon from the granulite facies septa (Zrc6, CD27) and from hornblende-rich amphibolite sample (Zrc1, CD49B). White circles and white dotted circles indicate locations of the analytical spots providing concordant and discordant U–Pb data, respectively. B) Tera-Wasserburg diagram showing zircon data from three analysed zircon grains, one from the septa and two from the hornblende-rich amphibolite. Only concordant data are reported in the inset and the discordia line between slightly discordant and concordant data from one zircon grain (Zrc1) observed within the hornblende-rich amphibolite is also shown. C) Back-Scattered Electrons images of a textural site containing the analysed monazite grains (Mnz2a-2d) forming an aggregate with biotite and apatite and surrounded by quartz and sillimanite (CD22 migmatite). D) Plot of $^{238}U/^{206}Pb$ and $^{232}Th/^{208}Pb$ monazite ages. Each couple of boxes refers to a specific analysis (see Table 1). Star indicates the concordance also between $^{238}U/^{206}Pb$ and the $^{235}U/^{207}Pb$ ages. E) and F) Tera-Wasserburg diagrams showing discordant titanite data from the CD27 septa and amphibolites (CD49A and CD34), respectively. Mineral abbreviations follow Kretz (1983).

Table 1. U-(Th)-Pb isotopic data of zircon, monazite and titanite.

2014, IGG-CNR U.O.S. of Pavia					Isotopic ratios							
Lithol.	Sample	Mineral	Identifier	Tex. Pos.	$^{207}Pb/^{206}Pb$	1s abs	$^{207}Pb/^{235}U$	1σ abs	$^{206}Pb/^{238}U$	1σ abs	$^{208}Pb/^{232}Th$	1σ abs
Hornblende-rich amphibolite	CD49B	Zrc	1a	in matrix	0,0704	0,0056	0,4755	0,0377	0,0492	0,0012		
	CD49B	Zrc	1b	in matrix	0,0534	0,0045	0,3291	0,0275	0,0450	0,0011		
	CD49B	Zrc	1c	in matrix	0,0590	0,0050	0,3936	0,0335	0,0479	0,0012		
	CD49B	Zrc	2a	in matrix	0,0573	0,0048	0,3583	0,0295	0,0454	0,0008		
	CD49B	Zrc	2b	in matrix	0,0691	0,0043	0,4230	0,0257	0,0444	0,0007		
	CD49B	Zrc	2c	in matrix	0,0654	0,0054	0,3988	0,0322	0,0446	0,0008		
Septa	CD27	Zrc	6a	*	0,0512	0,0037	0,3082	0,0222	0,0435	0,0009		
	CD27	Zrc	6b	*	0,0514	0,0031	0,2582	0,0154	0,0364	0,0007		
Migmatites	CD22	Mnz	1	in garnet	0,0617	0,0011	0,4285	0,0081	0,0504	0,0007	0,0158	0,0002
	CD22	Mnz	2a	in matrix	0,0517	0,0009	0,3114	0,0059	0,0438	0,0006	0,0137	0,0002
	CD22	Mnz	2a	in matrix	0,0516	0,0010	0,3165	0,0065	0,0443	0,0007	0,0130	0,0002
	CD22	Mnz	2b	in matrix	0,0537	0,0011	0,3126	0,0067	0,0422	0,0006	0,0119	0,0002
	CD22	Mnz	2b	in matrix	0,0519	0,0012	0,3158	0,0075	0,0441	0,0006	0,0125	0,0002
	CD22	Mnz	2c	in matrix	0,0514	0,0011	0,2516	0,0054	0,0356	0,0005	0,0106	0,0002
	CD22	Mnz	2d	in matrix	0,0516	0,0015	0,3095	0,0090	0,0435	0,0007	0,0115	0,0002
Plagioclase-rich amphibolites	CD34	Ttn	21	in matrix	0,1795	0,0117	1,0182	0,0644	0,0412	0,0012		
	CD34	Ttn	13	in matrix	0,2133	0,0155	1,2172	0,0838	0,0415	0,0014		
	CD34	Ttn	20	in matrix	0,2122	0,0131	1,2001	0,0716	0,0411	0,0012		
	CD34	Ttn	14	in matrix	0,3425	0,0236	2,2954	0,1449	0,0487	0,0018		
	CD34	Ttn	33	in matrix	0,2393	0,0164	1,5251	0,0984	0,0463	0,0015		
	CD34	Ttn	30a	in matrix	0,2050	0,0137	1,2306	0,0787	0,0436	0,0014		
	CD34	Ttn	30b	in matrix	0,2017	0,0157	1,1790	0,0868	0,0425	0,0015		
	CD34	Ttn	27	in matrix	0,1990	0,0137	1,2459	0,0821	0,0455	0,0014		
	CD34	Ttn	5	in matrix	0,2300	0,0265	1,3937	0,1476	0,0440	0,0023		
	CD34	Ttn	4	in matrix	0,3559	0,0339	2,4436	0,2066	0,0499	0,0026		
	CD34	Ttn	3b	in matrix	0,3059	0,0224	2,1017	0,1417	0,0499	0,0019		
	CD34	Ttn	2	in matrix	0,2125	0,0154	1,2820	0,0878	0,0438	0,0015		
	CD49A	Ttn	2	in matrix	0,5792	0,0483	5,7042	0,4044	0,0716	0,0037		
	CD49A	Ttn	10	in matrix	0,4099	0,0354	3,0763	0,2348	0,0544	0,0026		
	CD49A	Ttn	16a	in matrix	0,4662	0,0328	3,8361	0,2403	0,0597	0,0024		
	CD49A	Ttn	16b	in matrix	0,5004	0,0432	4,3563	0,3243	0,0631	0,0032		
Septa	CD27	Ttn	14c	in garnet	0,1148	0,0062	0,4794	0,0240	0,0303	0,0007		
	CD27	Ttn	18a	in garnet	0,1122	0,0054	0,4765	0,0209	0,0307	0,0006		
	CD27	Ttn	18b	in garnet	0,1200	0,0055	0,5210	0,0215	0,0314	0,0006		
	CD27	Ttn	13	in matrix	0,1420	0,0084	0,6508	0,0354	0,0331	0,0008		
	CD27	Ttn	12	in matrix	0,1514	0,0079	0,7383	0,0348	0,0353	0,0008		
	CD27	Ttn	10	in matrix	0,1303	0,0082	0,5728	0,0333	0,0318	0,0008		
	CD27	Ttn	21	in matrix	0,1252	0,0086	0,5674	0,0359	0,0327	0,0009		
	CD27	Ttn	9a	in matrix	0,1321	0,0088	0,6025	0,0368	0,0329	0,0009		
	CD27	Ttn	9b	in matrix	0,1465	0,0091	0,6524	0,0372	0,0322	0,0008		
	CD27	Ttn	5a	in matrix	0,1358	0,0071	0,6036	0,0286	0,0322	0,0007		
	CD27	Ttn	5b	in matrix	0,1240	0,0071	0,5238	0,0274	0,0305	0,0007		
	CD27	Ttn	5c	in matrix	0,1187	0,0063	0,5185	0,0253	0,0316	0,0007		
	CD27	Ttn	4	in matrix	0,1314	0,0079	0,5538	0,0306	0,0306	0,0007		
	CD27	Ttn	2a	in matrix	0,1491	0,0075	0,7332	0,0330	0,0357	0,0008		
	CD27	Ttn	2b	in matrix	0,1288	0,0072	0,5988	0,0303	0,0337	0,0008		
	CD27	Ttn	2c	in matrix	0,1452	0,0091	0,7089	0,0403	0,0354	0,0009		

Lithol. = lithology; Tex. Pos. = textural position (* indicates mineral analysed as separate); abs = absolute.

Table 1. Continued…

					Ages								Concordant data	
Lithol.	Sample	Mineral	Identifier	Tex. Pos.	$^{207}Pb/^{206}Pb$	1σ abs	$^{207}Pb/^{235}U$	1σ abs	$^{206}Pb/^{238}U$	1σ abs	$^{208}Pb/^{232}Th$	1σ abs	Age	2σ abs
Hornblende-rich amphibolite	CD49B	Zrc	1a	in matrix	939	75	395	31	310	8				
	CD49B	Zrc	1b	in matrix	346	29	289	24	284	7			284	14
	CD49B	Zrc	1c	in matrix	566	48	337	29	302	8				
	CD49B	Zrc	2a	in matrix	503	84	311	51	286	10				
	CD49B	Zrc	2b	in matrix	902	111	358	43	280	8				
	CD49B	Zrc	2c	in matrix	788	130	341	55	281	10				
Septa	CD27	Zrc	6a	*	252	18	273	20	275	6			275	11
	CD27	Zrc	6b	*	261	16	233	14	230	4			230	8
Migmatites	CD22	Mnz	1	in garnet	664	12	362	7	317	5	317	5		
	CD22	Mnz	2a	in matrix	270	5	275	5	276	4	276	4	276	8
	CD22	Mnz	2a	in matrix	268	5	279	6	280	4	260	4	280	8
	CD22	Mnz	2b	in matrix	358	7	276	6	266	4	240	4		
	CD22	Mnz	2b	in matrix	280	7	279	7	278	4	251	4	278	8
	CD22	Mnz	2c	in matrix	258	5	228	5	225	3	213	3	225	7
	CD22	Mnz	2d	in matrix	267	8	274	8	275	4	230	3	275	9

the U–Pb dates. Notwithstanding, available data on the septa and the hornblende-rich amphibolite suggests that the U–Pb system in zircon records a high temperature event at about 280 Ma. Its significance is however not clear. Permian dates may refer both to a crystallization and a recrystallization (reset) process. According to petrography, amphibolites have an igneous mafic protolith. Apparently, the oscillatory zoning of the zircon grains from the hornblende-rich amphibolite (Figure 5A) suggests an igneous origin, that would favour the interpretation of the Permian dates as crystallization ages. However, the apparently weak luminescence of the near homogeneous zircon grain from the granulitic septa do not allow to exclude that both the Permian and Triassic dates are metamorphic ages in response to a high temperature events.

Monazite grains from the migmatitic metapelite have complex U–Th–Pb age patterns. A single monazite grain included in garnet yielded a robust concordant $^{206}Pb/^{238}U$ – $^{208}Pb/^{232}Th$ date at 317±5 Ma. Considering the thermal shield action played by the host garnet during the successive high temperature events (e.g., Langone et al., 2011), this date is a good estimate of the age of the prograde metamorphism. Matrix monazite is in textural equilibrium with sillimanite and thus the U–Pb concordant dates at about 276 Ma likely refer to cooling after the metamorphic peak conditions. The U–Pb date at 225±7 Ma and the scattered Th-Pb dates between 280 Ma and 213 Ma reveal that a Triassic high temperature event interested the migmatitic metapelite. Remarkably, this event is coeval with that recorded by zircon in the septa.

Titanite U–Pb dates in the septa and in the plagioclase-rich amphibolites yield Jurassic and Triassic ages, respectively. Textural features in both rock types suggest that titanite growth occurred during prograde/peak metamorphic conditions, via dehydration reaction consuming hornblende and producing clinopyroxene and other mineral phases (plagioclase, hematite, quartz; e.g. Spear, 1981). Similar evidence was previously reported by Harlov et al. (2006) for the amphibolites in Val Strona. However, as titanite is very reactive during metamorphism (e.g. Frost et al., 2000), thermally mediated volume diffusion, (re)crystallization induced by fluid flow, deformation, or reaction (e.g. Spencer et al., 2013) may have induced resetting

of the U–Pb system. The Triassic and Jurassic lower intercept ages may thus not necessarily constrain the age of the titanite forming reaction (prograde/peak conditions). In addition, in the interpretation of titanite ages the unavailability of matrix matched external standard cannot be also neglected, as it may introduce errors as high as 12% (e.g. Sun et al., 2012). However, the consistence between Triassic ages from titanite, zircon and monazite apparently support the conclusions of Storey et al. (2006) that the method error introduced by using zircon as external standard is negligible.

In conclusion, by coupling the age results from the different geochronometers (zircon, monazite and titanite) applied to migmatitic metapelite, amphibolites and granulites (septa) from the northernmost sector of the IVZ we can recognize three high temperature events that affected the studied crustal section during lower Permian, Triassic and Jurassic. Their significance is discussed in the next section.

Tectono-metamorphic implications

The new field, petrographic and geochronological data of this study allow us to reconstruct and discuss, also in the frame of literature data, a possible tectono-metamorphic evolution from Permian to Jurassic for the investigated crustal sector of the IVZ (Figure 6).

Carboniferous-Permian

The single Carboniferous age found in monazite included in garnet of the migmatitic metapelite, interpreted to date the prograde metamorphism, perfectly agrees with the age of the regional amphibolite to granulite facies metamorphism of the IVZ at 316±3 Ma (Ewing et al., 2013). The northernmost sector of the IVZ seems thus to have evolved similarly to the rest of the IVZ until Carboniferous.

The Permian event (at about 280 Ma) recorded by hornblende-rich amphibolites and migmatitic metapelite from the Kinzigite Formation in the northernmost sector of the IVZ is well documented in the southern/central IVZ. Here, the lower crust experienced the intrusion of mafic magmas locally inducing contact metamorphism (e.g. Barboza et al., 1999; Barboza and Bergantz, 2000; Peressini et al., 2007; Redler et al., 2012; Ewing et al., 2013). The identification of a heat source for the Permian high temperature event in the northernmost sector of the IVZ is however not straightforward. A Permian Mafic Complex in the north-eastern sector of the IVZ is apparently missing (Figure 1B). Both the Layered Internal Zone and the External Gabbro units of the Finero Mafic Complex in Valle Cannobina (near Finero) yield Triassic ages (Lu et al., 1997; Zanetti et al., 2013). Note however, that Lu et al. (1997) interpreted the internal isochron Triassic ages in the Layered Internal Zone as the response to a regional heating event. Whereas, Zanetti et al. (2013) interpreted the Triassic U–Pb rim ages in zircon from the External Gabbro unit as crystallization ages. The only intrusives giving relatively well constrained Permian ages are those found at higher crustal levels of the Kinzigite Formation as sporadic dike swarms ("Apinnites") and coeval with the activity of the extensional CMBL (Boriani et al., 1990; Boriani et al., 1995; Mulch et al., 2002b). For the small volumes and the higher structural position this magmatic event is unlikely responsible for a regional scale high temperature event. Two alternatives can thus explain the high temperature event recorded by the Kinzigite Formation in Valle Cannobina. According to a first hypothesis a Permian magmatism (similar to that found in the southern IVZ, e.g. Peressini et al., 2007) would have been present at the base of the crust but its products are presently not (or only partially) exposed. The long lasted post Variscan extensional activity may have caused the tectonic elision of the Permian intrusive rocks and lower crustal granulites showing contact metamorphism. This hypothesis is supported by the mylonitic

deformation associated to the activity of the Pogallo Line at the contact between metabasic rocks of the Finero Mafic Complex and the metamorphic rocks of the Kinzigite Formation (Figure 6). Alternatively, in order to explain the thermal perturbation at 280 Ma found in the Kinzigite Formation, a Permian age of the Finero Mafic Complex (or part of it) has to be supposed. Support to this hypothesis comes from the growing geochemical evidence that the Layered Internal Zone is petrogenetically unrelated to the External Gabbro unit (e.g. Langone et al., 2013). Further support is also given by the occurrence of an high temperature shear zone separating the

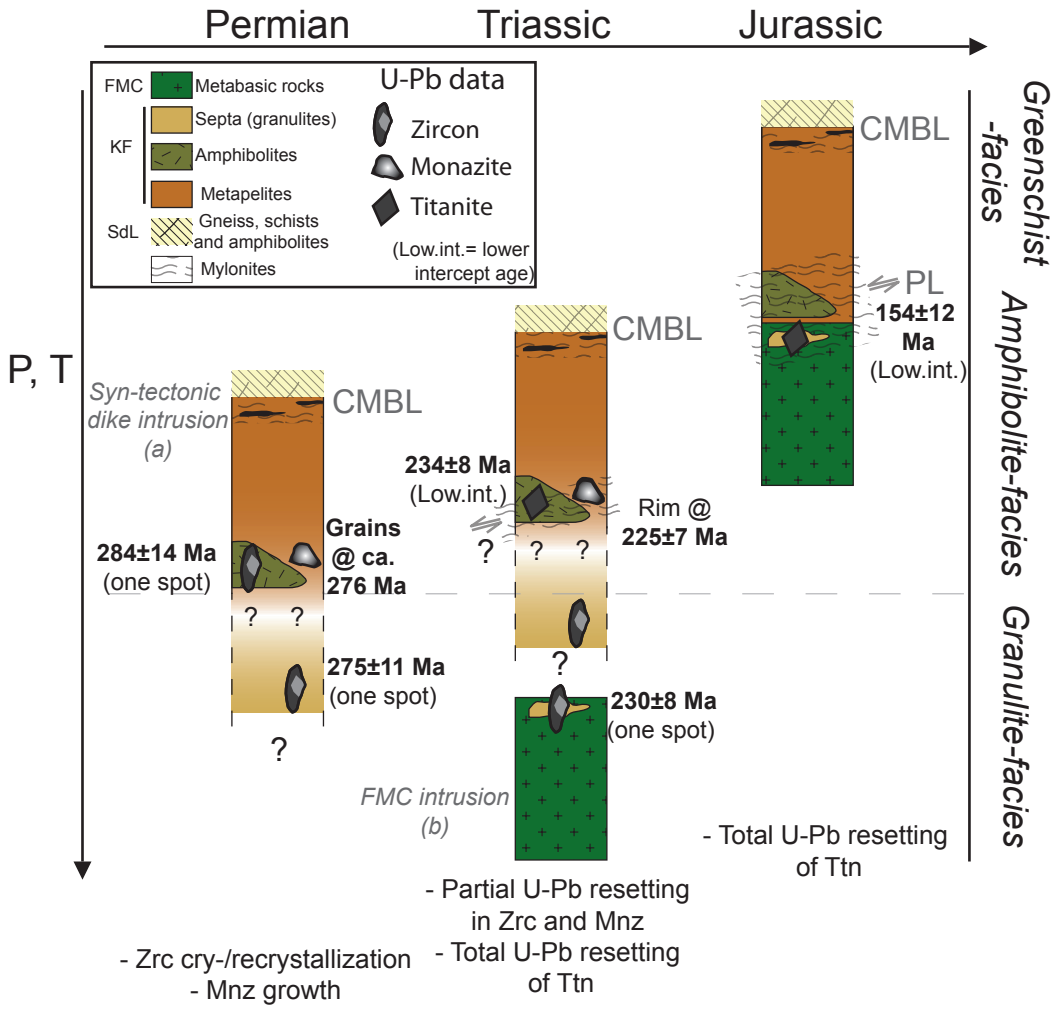

Figure 6. Permian-Jurassic reconstruction of the IVZ exposed in Valle Cannobina. The crustal boxes (not in scale) would represent the crustal section and the main tectono-metamorphic and magmatic events, based on new geochronological data and previous studies. (a) Mulch et al. (2002b); (b) Zanetti et al. (2013).

two units (e.g. Kenkmann, 2000). The Layered Internal Zone may be thus an analogous of the Mafic Complex of the central/southern IVZ intruded by or tectonically juxtaposed to the Triassic External Gabbro unit in more recent times. In this case the Triassic ages reported by Lu et al. (1997) for the Layered Internal Zone would be easily interpreted as the response to the intrusion of the External Gabbro unit. A more detailed geochronological characterization of the deformation and of the Layered Internal Zone is however required to better constrain this argument.

Triassic

Triassic ages are relatively common in the analysed rocks and, in both monazite and zircon, likely represent a high temperature perturbation event (fluid mediated) superimposed to that occurred during Permian. The Triassic event has completely elided any previous geochronological record in titanite from the plagioclase-rich amphibolites.

During Triassic time the IVZ was affected by extension, thinning and tilting (e.g. Handy, 1987, Zingg et al., 1990; Wolff et al., 2012) and crustal scale shear zones (e.g. the Pogallo Line) were active. Remarkably, several geochronometers record the Triassic time in the form of alteration domains due to fluid-rock interaction (Vavra and Schaltegger 1999; Vavra et al., 1999; Zanetti et al., 2013). According to Zanetti et al. (2013) the northernmost sector of the IVZ, experienced during Triassic the intrusion of the mafic melts at the origin of the External Gabbro unit. After the emplacement, the External Gabbro unit however recorded a metamorphic overprint in granulite facies conditions (e.g. Kenkmann, 2000) and ductile deformation (Figure 6).

Presently the original intrusive relations between the Kinzigite Formation and the External Gabbro unit are not preserved and we do not know the structural position of the Kinzigite Formation at the time of the intrusion of the External Gabbro unit. However, the link between the Triassic ages from the plagioclase-rich amphibolites and the intrusion of the External Gabbro unit is apparently straightforward. Fluids released from the cooling magma (and the contact aureole?) that reached the presently exposed rocks of the Kinzigite Formation, promoting titanite (re)crystallization and U–Pb resetting, is the favoured hypothesis (Figure 6). Plagioclase-rich amphibolites show however also a mylonitic deformation that does not allow to exclude that fluid circulation along shear planes, prodromes of the Pogallo Line, promoted the reset of the U–Pb system in titanite.

Jurassic

Jurassic ages are peculiar of titanite from the mafic granulitic septa. Here, the discordance among titanite and zircon U–Pb ages is too high to be related to the different closure temperatures of the two chronometers. Titanite thus likely records a Jurassic event that was not efficient in resetting zircon in the same rock. A Jurassic thermal pulse was suggested by Smye and Stockily (2014) based on U–Pb dating of rutile from the high grade metamorphic rocks (granulites) of the Kinzigite Formation in the central and southern part of the IVZ. According to these authors a regional scale thermal pulse affected the lower structural levels of the IVZ in response to the hyperextension of the Adriatic margin. Rutile Jurassic ages at about 175 and 160 Ma from granulite facies metapelites of the central and southern part of the IVZ were interpreted by Ewing et al. (2015) as cooling ages associated with rift-/post-rift processes at the Adriatic margin. Remarkably, Jurassic U–Pb ages were also reported for metamorphic titanite from a granitic dike intruded into the upper structural levels of the Kinzigite Formation. Here, however, they were interpreted as ages of retrograde metamorphic reactions associated with crustal attenuation localized along the

Pogallo Line (Mulch et al., 2002b). Even though the activity of the Pogallo shear zone is still not well-constrained, current geochronological data of mylonites point to middle/lower Jurassic ages (e.g. in situ Ar-Ar mica dating, Mulch et al., 2002a). The absence of Jurassic ages in the titanite of the amphibolites is crucial for the interpretation of the most recent evolution of the northernmost sector of the IVZ. The Jurassic thermal pulse was localized in the septa and was not efficient in resetting titanite from the plagioclase-rich amphibolites of the Kinzigite Formation. In the studied area the activity of the Pogallo Line have deeply affected the lithologies of the External Gabbro unit and the enclosed septa, giving a mylonitic fabric (Figs. 4D and 6). However, it only marginally interested the amphibolites and the metapelites of the Kinzigite Formation. This evidence thus strongly supports the origin of the Jurassic ages in titanite of the septa as related to high temperature fluid circulation during the activity of amphibolite facies shear zones (i.e. Pogallo Line).

Conclusions

Based on field and petrographic observations, the Kinzigite Formation in the northernmost sector of the IVZ (Valle Cannobina) consists of siliciclastic metasediments and amphibolites showing a metamorphic gradient from amphibolite to upper amphibolite facies that slightly increases from SE towards NW. Granulite facies conditions are recorded only in small bodies/lenses of metamorphic rocks (septa) enclosed in the External Gabbro unit of the Finero Mafic Complex and likely belonging to the Kinzigite Formation. Septa were affected also by a ductile deformation leading to a well developed mylonitic to ultramylonitic fabric.

U–(Th)–Pb dating of different accessory minerals from different rock types of the Kinzigite Formation allowed recognizing at least three discrete tectono-metamorphic events. Zircon from the lowest structural levels and monazite from the migmatitic metapelite indicate a major high temperature event during Permian at about 280 Ma. This event is likely related to the intrusion of mafic melts, whose products are possibly not exposed in the northernmost sector of the IVZ. Titanite and recrystallized zircon and monazite domains recorded a Triassic event. Triassic ages are possibly related to the thermal effect and fluid circulation during the emplacement of the External Gabbro unit. However, we cannot exclude that they are the response to the onset of ductile deformation along the Pogallo Line, which protracted until Jurassic. This Jurassic activity along the Pogallo Line is well-recorded by titanite from the granulitic septa showing mylonitic deformation. Most likely, fluid circulation along the mylonitic planes promoted the U–Pb reseting of titanite.

Our new results, even though preliminary and thus not fully conclusive, are robust, self consistent and in agreement with previous published data available for the investigated area and more in general for the entire IVZ. According to the new geochronological data we conclude that the investigated sector of the IVZ shares strong similarities with the other sectors of the IVZ, e.g. the presence of high temperature events and deformation during Permian and Jurassic. However, the Kinzigite Formation exposed in Valle Cannobina shows a peculiar Triassic tectono-metamorphic event whose origin is still mater of debate.

This study is a further evidence that geochronology of crystalline basements must be approached coupling geochronometers with different reactivity as function of the bulk composition and metamorphic conditions.

Acknowledgements

Alberto Zanetti, Maurizio Mazzucchelli and Tommaso Giovanardi are gratefully acknowledged for stimulating discussions. We

thank Charlotte Redler, Francesca Micheletti and the guest editor Michele Zucali for their constructive comments that improved the manuscript. Carlo Bergamaschi and Davide Berno provided generous support with geological mapping, sample preparation, petrography and isotopic analyses.

References

Barboza S.A. and Bergantz G.W. (2000) - Metamorphism and anatexis in the mafic complex contact aureole, Ivrea zone, northern Italy. *Journal of Petrology,* 41, 1307-1327.

Barboza S.A., Bergantz G.W. and Brown M. (1999) - Regional granulite facies metamorphism in the Ivrea Zone: Is the Mafic Complex the smoking gun or red herring? *Geology*, 27, 447-450.

Bertolani M. (1968) - La petrografia della Valle Strona (Alpi Occidentali Italiane). S*chweizer Mineralogische und Petrographische Mitteilungen*, 48, 695-732.

Boriani A. and Burlini L. (1995) - Carta geologica della Valle Cannobina. Scala 1:25000. Comunità montana Valle Cannobina, Dipartimento di Scienze della Terra dell'Università degli Studi di Milano, Centro di Studio per la geodinamica Alpina e Quaternaria del CNR-Milano. Grafiche Diodoro, Milano.

Boriani A. and Sacchi R. (1973) - Geology of the junction between the Ivrea-Verbano and Strona-Ceneri Zones. *Memorie dell'Istituto Geologico e Mineralogico Università di Padova*, 28, 36 pp.

Boriani A., Burlini L. and Sacchi R. (1990) - The Cossato-Mergozzo-Brissago Line and the Pogallo Line (southern Alps, Northern Italy) and their relationships with the late-Hercynian magmatic and metamorphic events. *Tectonophysics*, 182, 91-102.

Boriani A.C. and Villa I.M. (1997) - Geochronology of regional metamorphism in the Ivrea-Verbano Zone and Serie dei Laghi, Italian Alps. *Schweizerische Mineralogische und Petrographische Mitteilungen,* 77, 381-401.

Burlini L. and Caironi V. (1988) - Geochemical and petrographical data on the Quarna pluton (Serie dei Laghi, Northern Italy). *Rendiconti Società Italiana Mineralogia Petrologia*, 43, 429-444.

Cherniak D.J. (1993) - Lead diffusion in titanite and preliminary results on the effects of radiation damage on Pb transport. *Chemical Geology*, 110, 177-194.

Compston W. (1999) - Geological age by instrumental analysis: the 29th Hallimond Lecture. *Mineralogical Magazine,* 63, 297-311.

Demarchi G., Quick J., Sinigoi S. and Mayer A. (1998) - Pressure gradient and original orientation of a lower-crustal intrusion in the Ivrea-Verbano Zone, northern Italy. *Journal of Geology* 5, 609-621.

Ewing T.A., Hermann J. and Rubatto D. (2013) - The robustness of the Zr-in-rutile and Ti-in zircon thermometers during high-temperature metamorphism (Ivrea-Verbano Zone, northern Italy). *Contributions to Mineralogy and Petrology,* 165, 757-779.

Ewing T.A., Rubatto D., Beltrandi M. and Hermann J. (2015) - Constraints on the thermal evolution of the Adriatic margin during Jurassic continental break-up: U–Pb dating of rutile from the Ivrea-Verbano Zone, Italy. *Contributions to Mineralogy and Petrology*, 169, DOI 10.1007/s00410-015-1135-6.

Frost B.R., Chamberlain K.R., Schumacher J.C., Scott D.J. and Moser D.E. (2000) - Sphene (titanite); phase relations and role as a geochronometer. *Chemical Geology,* 172, 131-148.

Gasquet D., Bertrand J.M., Paquette J.L., Lehmann J., Ratzov G., De Ascenção Guedes R., Tiepolo M., Boullier A.M., Scaillet S. and Nomade, S. (2010) - Miocene to Messinian deformation and hydrothermal activity in a pre-Alpine basement massif of the French western Alps: new U–Th–Pb and argon ages from the Lauzière massif. *Bulletin de la Société Géologique de France,* 181, 227-241.

Handy M.R., (1987) - The structure, age and kinematics of the Pogallo fault zone-Southern Alps, northwestern Italy. *Eclogae Geologicae Helvetiae*, 80, 593-632.

Handy M.R. and Zingg A. (1991) - The tectonic and rheological evolution of an attenuated cross section of the continental crust: Ivrea crustal section, southern Alps, northwestern Italy and southern Switzerland. *Geological Society of American Bulletin*, 103, 236-253.

Harlov D. and Förster H.J. (2002a) - High-Grade Fluid Metasomatism on both a Local and Regional Scale: the Seward Peninsula, Alaska and the Val Strona di Omegna, Ivrea-Verbano Zone, Northern Italy. Part I: Petrography and Silicate Mineral Chemistry. *Journal of Petrology*, 43, 769-799.

Harlov D. and Förster H.J. (2002b) - High-Grade Fluid

Metasomatism on both a Local and Regional Scale: the Seward Peninsula, Alaska and the Val Strona di Omegna, Ivrea-Verbano Zone, Northern Italy. Part II: Phosphate Mineral Chemistry. *Journal of Petrology*, 43, 801-824.

Harlov D., Tropper P., Seifert W., Nijland T. and Förster H.J. (2006) - Formation of Al-rich titanite ($CaTiSiO_4O$-$CaAlSiO_4OH$) reaction rims on ilmenite in metamorphic rocks as a function of fH_2O and fO_2. *Lithos*, 88, 72-84.

Henk A., Franz L., Teufel S. and Oncken O. (1997) - Magmatic underplating, extension and crustal reequilibration: insights from a cross-section through the Ivrea Zone and Strona-Ceneri Zone, Northern Italy. *Journal of Geology,* 105, 367-377.

Hiess J., Condon D.J. McLean N. and Noble S.R. (2012) - $^{238}U/^{235}U$ systematics in terrestrial Uranium-bearing minerals. *Geology,* 335, 1610-1614.

Hodges K.V. and Fountain D.M. (1984) - Pogallo Line, South Alps, northern Italy: an intermediate crystal level, low-angle normal fault? *Geology*, 12, 151-155.

Horstwood M.S.A., Foster G.L., Parrish R.R., Noble S.R. and Nowell G.M. (2003) - Common-Pb corrected in situ U–Pb accessory mineral geochronology by LA–MC–ICP–MS. *Journal of Analytical Atomic Spectrometry,* 18, 837-846.

Jackson S.E., Pearson N.J., Griffin W.L. and Belousova E. (2004) - The application of laser ablation inductively coupled plasma mass spectrometry to in situ U–Pb zircon geochronology. *Chemical Geology*, 211, 47-69.

Kenkmann T. (2000) - Processes controlling the shrinkage of porphyroclasts in gabbroic shear zones. *Journal of Structural Geology,* 22, 471-487.

Kretz R. (1983) - Symbols for rock-forming minerals. *American Mineralogist,* 68, 277-279.

Kunz B.E., Johnson T.E., White R.W. and Redler C. (2014) - Partial melting of metabasic rocks in Val Strona di Omegna, Ivrea Zone, northern Italy. *Lithos*, 190-191, 1-12.

Langone A., Braga R., Massonne H.J. and Tiepolo M. (2011) - Preservation of old (prograde metamorphic) U–Th–Pb ages in unshielded monazite from the high-pressure paragneisses of the Variscan Ulten Zone (Italy). *Lithos*, 127, 68-85.

Langone A., Renna M.R., Tiepolo M., Zanetti A., Mazzucchelli M. and Giovanardi T. (2013) - New insights into the evolution of the Finero Mafic Complex. Goldschmidt 2013 Conference Abstracts, *Mineralogical Magazine*, 1545.

Lu M., Hofman A.W., Mazzucchelli M. and Rivalenti G. (1997) - The mafic-ultramafic complex near Finero (Ivrea-Verbano Zone), II Geochronology and isotope geochemistry. *Chemical Geology*, 140, 223-235.

Ludwig K.R. (2003) - Isoplot/Ex version 3.0: a geochronological toolkit for Microsoft Excel. *Berkeley Geochronology Center Special Publication 4*. Berkeley, Berkeley Geochronology Center, 70 p.

Mulch A., Cosca M.A. and Handy M.R. (2002a) - In-situ UV-laser 40Ar/39Ar geochronology of a micaceous mylonite: an example of defect enhanced argon loss. *Contributions to Mineralogy and Petrology,* 142, 738-752.

Mulch A., Rosenau M., Dörr W. and Handy M.R. (2002b) - The age and structure of dikes along the tectonic contact of the Ivrea-Verbano and Strona-Ceneri Zones (southern Alps, Northern Italy, Switzerland). *Schweizerische Mineralogische und Petrographische Mitteilungen,* 82, 55-76

Paquette J.L. and Tiepolo M. (2007) - High resolution (5 mm) U–Th–Pb isotope dating of monazite with excimer laser ablation (ELA)-ICPMS. *Chemical Geology,* 240, 222-237.

Peressini G., Quick J.E., Sinigoi S., Hofmann A.W. and Fanning M. (2007) - Duration of a Large Mafic Intrusion and Heat Transfer in the Lower Crust: a SHRIMP U–Pb Zircon Study in the Ivrea-Verbano Zone (Western Alps, Italy). *Journal of Petrology,* 48, 1185-1218.

Quick J.E., Sinigoi S., Snoke A.W., Kalakay T.J., Mayer A. and Peressini G. (2003) - Geologic map of the southern Ivrea-Verbano Zone, Northwestern Italy: U.S. Geological Survey, Geologic Investigations Series Map I-2776, scale 1:25,000, 22p.

Redler C., Johnson T.E., White R.W. and Kunz B.E. (2012) - Phase equilibrium constraints on a deep crustal metamorphic field gradient: metapelitic rocks from the Ivrea Zone (NW Italy). *Journal of Metamorphic Geology,* 30, 235-254.

Rivalenti G., Garuti G. and Rossi A. (1975) - The origin of the Ivrea-Verbano basic formation (western Italian Alps); whole rock geochemistry. *Bollettino della Società Geologica Italiana*, 94, 1149-1186.

Rubatto D., Gebauer D. and Compagnoni R. (1999) - Dating of eclogite-facies zircons: the age of Alpine metamorphism in the Sesia-Lanzo Zone (Western Alps). *Earth Planetary Science Letters*, 167, 141-

158.

Schaltegger U. and Gebauer D. (1999) - Pre-Alpine geochronology of the Central, Western and Southern Alps. *Schweizerische Mineralogische und Petrographische Mitteilungen*, 79, 79-87.

Schaltegger U., Ulianov A., Muntener O., Ovtcharova M., Peytcheva I., Vonlanthen P., Vennemann T., Antognini M. and Girlanda F. (2015) - Megacrystic zircon with planar fractures in miaskite-type nepheline pegmatites formed at high pressures in the lower crust (Ivrea Zone, southern Alps, Switzerland). *American Mineralogist*, 100, 83-94.

Schmid S.M. (1993) - Ivrea zone and adjacent southern Alpine basement. In: Pre-Mesozoic Geology in the Alps. (eds): J.F. von Raumer and F. Neubauer, Springer-Verlag, Berlin, pp. 567-583.

Schmid R., Wood B.J. (1976) - Phase relationships in granulitic metapelites from the Ivrea-Verbano zone (Northern Italy). *Contributions to Mineralogy and Petrology,* 54, 255-279.

Schmid S.M., Zingg A. and Handy M. (1987) - The kinematics of movements along the Insubric Line and the emplacement of the Ivrea Zone. *Tectonophysics,* 135, 47-66.

Schnetger B. (1994) - Partial melting during the evolution of the amphibolite-facies to granulite-facies gneisses of the Ivrea Zone, northern Italy. *Chemical Geology,* 113, 71-101.

Seydoux-Guillaume A.M., Paquette J.L., Wiedenbeck M., Montel J.M. and Heinrich W. (2002a) - Experimental resetting of the U–Th–Pb system in monazite. *Chemical Geology,* 191, 165-181.

Seydoux-Guillaume A.M., Wirth R., Nasdala L., Gottschalk M., Montel J.M. and Heinrich W. (2002b) - XRD, TEM and Raman study of experimental annealing of natural monazite. *Physics and Chemistry of Minerals,* 29, 240-253.

Siena F. and Coltorti M. (1989) - The petrogenesis of a hydrated mafic-ultramafic complex and the role of amphibole fractionation at Finero (Italian Western Alps). *Neues Jahrbuch für Mineralogie*, 6, 255-274.

Sinigoi S., Quick J.E., Clemens-Knott D., Mayer A., Demarchi G., Mazzucchelli M., Negrini L. and Rivalenti G. (1994) - Chemical evolution of a large mafic intrusion in the lower crust, Ivrea-Verbano Zone, northern Italy. *Journal of Geophysical Research: Solid Earth*, 99, 21575-21590.

Sinigoi S., Quick J.E., Mayer A. and Budahn J. (1996) - Influence of stretching and density contrasts on the chemical evolution of continental magmas: an example from the Ivrea-Verbano zone. *Contributions to Mineralogy and Petrology,* 123, 238-250.

Smye A.J. and Stockli D.F. (2014) - Rutile U–Pb depth profiling: A continuous record of lithospheric thermal evolution. *Earth Planetary Science Letters,* 408, 171-182.

Spear F.S. (1981) - An experimental study of hornblende stability and compositional variability in amphibole. *American Journal of Science*, 281, 697-734.

Spencer K.J., Hacker B.R., Kylander-Clark A.R.C., Andersen T.B., Cottle J.M., Stearns M.A., Poletti J.E. and Seward G.G.E. (2013) - Compaign-style titanite U–Pb dating by laser-ablation ICP: implications for crustal flow, phase transformations and titanite closure. *Chemical Geology,* 341, 84-101.

Storey C.D., Jeffries T.E. and Smith M. (2006) - Common lead corrected laser ablation ICP-MS systematics and geochronology of titanite. *Chemical Geology,* 227, 37-52.

Sun J.F., Yang J.H., Wu F.Y., Xie L.W., Yang Y.H., Liu Z.C. and Li X.H. (2012) - In situ U–Pb dating of titanite by LA-ICPMS. *Chinese Science Bulletin*, 57, 2506-2516.

Tera F. and Wasserburg J. (1972) - U–Th–Pb systematics in three Apollo 14 basalts and the problem of initial Pb in lunar rocks. *Earth Planetary Science Letters,* 14, 281-304.

Tiepolo M., Bottazzi P., Palenzona M. and Vannucci R. (2003) - A laser probe coupled with ICP-double focusing sector-field mass spectrometer from in situ analysis of geological samples and U–Pb dating of zircon. *The Canadian Mineralogist,* 41, 259-272.

Van Achterbergh E., Ryan C.G., Jackson S.E. and Griffin W. (2001) - Data reduction software for LA-ICPMS. In Sylvester, P., ed. Laser ablation ICPMS in the earth sciences: principles and applications. *Mineralogical Association of Canada Short Course Ser*. 29, 239-243.

Vavra G. and Schaltegger U. (1999) - Post-granulite facies monazite growth and rejuvenation during Permian to Lower Jurassic thermal and fluid events in the Ivrea Zone (Southern Alps). *Contributions to Mineralogy and Petrology,* 134, 405-414.

Vavra G., Schmid R. and Gebauer D. (1999) - Internal morphology, habit and U–Th–Pb microanalysis of amphibolite-to-granulite facies zircons: geochronology of the Ivrea Zone (Southern Alps). *Contributions to Mineralogy and Petrology,* 134,

380-404.

Voshage H., Hunziker J.C., Hofmann A.W. and Zingg A. (1987) - A Nd and Sr isotopic study of the Ivrea Zone, Southern Alps, N-Italy. *Contributions to Mineralogy and Petrology*, 97, 31-42.

Wiedenbeck M., Allé P., Corfu F., Griffin W.L., Meier M., Oberli F., Von Quadt A., Roddick J.C. and Spiegel W. (1995) - Three natural zircon standards for U–Th–Pb, Lu–Hf, trace elements and REE analyses. *Geostandards Newsletter*, 19, 1-23.

Wolff R., Dunkl I., Kiesselbach G., Wemmer K. and Siegesmund S. (2012) - Thermochronological constraints on the multiphase exhumation history of the Ivrea-Verbano Zone of the southern Alps. *Tectonophysics*, 579, 104-117.

Zanetti A., Mazzucchelli M., Rivalenti G. and Vannucci R. (1999) - The Finero phlogopite-peridotite massif: an example of subduction-related metasomatism. *Contributions to Mineralogy and Petrology,* 134, 107-122.

Zanetti A., Mazzucchelli M., Sinigoi S., Giovanardi T., Peressini G. and Fanning M. (2013) - SHRIMP U–Pb zircon Triassic intrusion age of Finero Mafic Complex (Ivrea-Verbano Zone, Western Alps) and its geodynamic implications. *Journal of Petrology*, 54, 2235-2265.

Zingg A. (1983) - The Ivrea and Strona-Ceneri Zones (Southern Alps, Ticino and N-Italy) - a review. *Schweizer Mineralogische und Petrographische Mitteilungen,* 63, 361-392.

Zingg A., Handy M.R., Hunziker J.C., Schmid S.M. (1990) - Tectonometamorphic history of the Ivrea Zone and its relationship to the crustal evolution of the Southern Alps. *Tectonophysics,* 182, 169-192.

Submitted, March 2015 - Accepted, October 2015